ELSEVIER

Journal of Nuclear Materials 300 (2002) 237–241

journal of nuclear materials

www.elsevier.com/locate/jnucmat

Thermodynamic stability of Na_2ZrO_3 using the solid electrolyte galvanic cell technique

R. Subasri, T. Mathews, K. Swaminathan, O.M. Sreedharan *

Thermodynamics and Kinetics Division, Materials Characterization Group, Indira Gandhi Centre for Atomic Research, Kalpakkam, Tamil Nadu 603 102, India

Received 6 August 2001; accepted 26 October 2001

Abstract

The sodium potential in the test electrode (a) $Pt, O_2, Na_2ZrO_3, ZrO_2$ was measured by using the emf technique employing Na-β″-alumina as the solid electrolyte in conjunction with (b) $Pt, O_2, Al_2O_3, NaAl_{11}O_{17}$, (c) $Pt, O_2, Na_2MoO_4, Na_2Mo_2O_7$ and (d) Pt, Na_2CO_3, CO_2, O_2 as the reference electrodes over the ranges 880–1045, 700–800 and 850–940 K, respectively. The emf results between electrodes (b) and (c) were utilized for internal consistency checks. From the results on cells formed between (a) and (b) and those on (a) and (c), the standard Gibbs energy of formation, $\Delta_f G^\circ$ (kJ/mol) of Na_2ZrO_3 was determined to be $-1699.4 + 0.3652T$ (K) valid over the temperature range 700–1045 K. The break in the emf data at 1045 K was corroborated by independent TG/DTA measurements carried out on Na_2ZrO_3 which exhibited an endotherm at 1055 K indicative of a phase transition in Na_2ZrO_3.

1. Introduction

Zirconium was reported to be one among the predominant fission products in fast breeder reactors wherein it was found to occur in the fluorite matrix of mixed oxide fuels and as $BaZrO_3$ in the perovskite type grey inclusions of irradiated fuels [1]. Hence, for an assessment of the relative stabilities of zirconates of alkaline-earth and alkali metals, it was considered necessary to build up a reliable thermodynamic database to cater to which objective, the present investigation was undertaken. Though there were a few investigations already reported in the literature by employing diverse techniques such as calorimetry [2], solid-state potentiometry [3], CO_2-manometry [4] and by theoretical estimation [5], the magnitude of scatter in the data would make another independent set of measurements desirable. Maier and Warhus [3] made emf measurements using Na-β-alumina ($NaAl_{11}O_{17}$) as the solid electrolyte over the range 600–1100 K. Beyer et al. [2] measured the enthalpy of formation of Na_2ZrO_3 over a wide span of temperature namely 5–1168 K by adiabatic calorimetry (5–305 K) and differential scanning calorimetry (438–1168 K) and reported a non-isothermal phase transition over the range 1025–1110 K. However, Maier and Warhus did not identify any phase transition in their emf measurements whose temperature range 600–1100 K encompassed the reported temperature of transition. The solid electrolyte galvanic cell technique, wherever applicable, is known to yield more precise Gibbs energy of formation data than any other technique and is generally amenable to reversibility and internal consistency checks. However, the standard enthalpy or entropy of formation data derived from solid electrolyte emf studies may not be reliable especially on electrodes bearing ternary oxides unless counterchecked by calorimetry.

Since there is only one set of measurements reported so far in the literature, that too employing a single

---

* Corresponding author. Tel.: +91-4114 80 202; fax: +91-4114 80 081.

E-mail address: oms@igcar.ernet.in (O.M. Sreedharan).

PII: S0022-3115(01)00734-6

reference electrode (Na_2CO_3, CO_2, O_2), another independent set of measurements was deemed as necessary. With a view to generating an internally consistent set of Gibbs energy data and for exploring the detectability of a not-so-reversible phase-transition in Na_2ZrO_3, the present investigation was undertaken.

2. Experimental

2.1. Synthesis

All chemicals used were of purity better than 99.9%. Na_2ZrO_3 was synthesized by a new polymeric gel combustion (PGC) method. Aqueous solutions of sodium nitrate and zirconyl nitrate were mixed in an appropriate proportion so as to synthesize Na_2ZrO_3 and homogenized at 360 K. Citric acid was added to this solution such that the ratio of the number of moles of citric acid to the total number of moles of the cations was 3:1. Ethylene glycol (the number of moles of which equaled half that of citric acid) was then added and the resultant solution left undisturbed at 353 K to facilitate gelation. The gel so formed was subsequently decomposed at 973 K. The powder X-ray diffraction (XRD) pattern of the decomposed gel showed the presence of Na_2ZrO_3 along with ZrO_2 and some unidentified peaks (could be due to a hydrated form of Na_2O). Hence, in order to ensure the completion of reaction, this powder was compacted into disks and heat treated at 1523 K for 3 h in a platinum crucible (which was closed to minimize volatilization of Na_2O). The XRD pattern of the heat-treated sample confirmed presence of pure Na_2ZrO_3 with traces of ZrO_2 whose presence would assist the emf measurements by realizing the phase boundary composition thereby eliminating the possible interference due to free Na_2O, if any. A thermoanalyzer, model Seiko 320, was employed to scan the DTA curve for a pellet of Na_2ZrO_3 of 6 mm diameter and 0.5 mm thickness (compacted at 200 MPa) in air at a linear heating rate of 10 K/min. The cooling was also traced to ascertain the reversibility of the phase transition.

2.2. Cell arrangement

Emf measurements were carried out as a function of temperature on the galvanic cells bearing the following configurations

$$(-)\mathrm{Pt}, O_2, Na_2ZrO_3, ZrO_2|\text{Na-}\beta''\text{-alumina}| \\ Al_2O_3, NaAl_{11}O_{17}, O_2, \mathrm{Pt}(+) \qquad (I)$$

$$(-)\mathrm{Pt}, O_2, Al_2O_3, NaAl_{11}O_{17}|\text{Na-}\beta''\text{-alumina}| \\ Na_2Mo_2O_7, Na_2MoO_4, O_2, \mathrm{Pt}(+) \qquad (II)$$

$$(-)\mathrm{Pt}, O_2, Na_2ZrO_3, ZrO_2|\text{Na-}\beta''\text{-alumina}| \\ Na_2Mo_2O_7, Na_2MoO_4, O_2, \mathrm{Pt}(+) \qquad (III)$$

$$(-)\mathrm{Pt}, O_2, CO_2, Na_2CO_3|\text{Na-}\beta''\text{-alumina}| \\ Na_2ZrO_3, ZrO_2, O_2, \mathrm{Pt}(+) \qquad (IV)$$

The sign of the electrodes in cells I–IV are indicated within parentheses. The overall virtual cell reaction for the galvanic cells I–IV corresponding to two faraday of electricity after correcting for the standard state of CO_2 in the case of cell IV are

$$Na_2ZrO_3\ (s) + 11Al_2O_3\ (s) \\ = 2NaAl_{11}O_{17}\ (s) + ZrO_2\ (s) \qquad (1)$$

$$Na_2Mo_2O_7\ (s) + 2NaAl_{11}O_{17}\ (s) \\ = 11Al_2O_3\ (s) + 2Na_2MoO_4\ (s) \qquad (2)$$

$$Na_2Mo_2O_7\ (s) + Na_2ZrO_3\ (s) \\ = 2Na_2MoO_4\ (s) + ZrO_2\ (s) \qquad (3)$$

and

$$Na_2CO_3\ (s) + ZrO_2\ (s) = Na_2ZrO_3\ (s) + CO_2\ (g), \qquad (4)$$

respectively. The reference electrodes are $\alpha\text{-}Al_2O_3 + NaAl_{11}O_{17}$ (Na-β-alumina) abbreviated as ASBA/O_2 ($p_{O_2} = 1.013$ bar), $Na_2MoO_4/Na_2Mo_2O_7/O_2$ ($p_{O_2} = 1.013$ bar) and $Na_2CO_3/CO_2/O_2$ ($p_{O_2} = 0.211$ bar). Na_2MoO_4 and $Na_2Mo_2O_7$ were synthesized through a solid-state route using Na_2CO_3 and MoO_3 in appropriate mole ratios. The details of the synthesis are given elsewhere [6]. A sintered pellet of Na_2CO_3 (Na_2CO_3 compacted at 300 MPa and sintered at 1023 K) was used as the reference electrode for one set of measurements. The test electrode was made by compacting an equimolar ratio of Na_2ZrO_3 and ZrO_2 for one set of runs on cells I and III (as given below) and with a 10 mol% nominal variation in the mole ratio for another set as part of testing the equilibrium nature of emf readings. The details of powder compaction, dimensions of the disk etc. are described in an earlier paper [7]. No such variation in composition was attempted for the reference electrodes ASBA and molybdates by conforming to the mole ratio of components, which yielded best results in earlier studies. An open-cell-stacked-pellet assembly as described in Ref. [8] was made use of for the emf measurements. A dense (higher than 98% theoretical density) Na^+ conducting MgO stabilized Na-β″-alumina ($Na_{1.67}Mg_{0.67}Al_{10.33}O_{17}$) disk of 15 mm diameter and 2 mm thickness was used as the solid electrolyte. The temperature measurements were made with a type-S thermocouple calibrated as per IPTS 68. Other experimental details including the micropolarization tests are the same as in our earlier publication [8]. The temperature dependence of the emf of cells I–IV was measured over the ranges 880–1045, 740–800, 700–800 and 850–940 K, respectively, in a flow of dry oxygen ($p_{O_2} = 1.013$ bar) for cells I–III. In the case of cell IV, convective air was employed in the ambience whose CO_2 content was assessed to be 305 ppm separately.

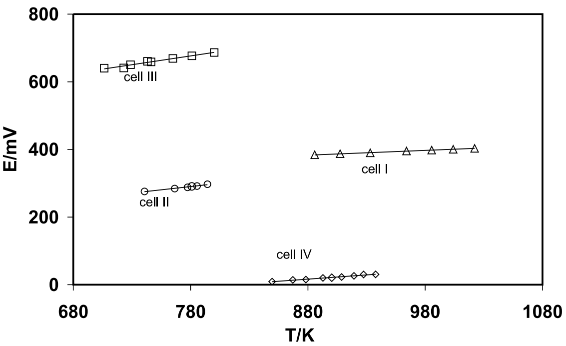

Fig. 2. Temperature dependence of the emf of cells I–IV.

Table 1
Coefficients of linear fit of emf–temperature data obtained for cells I–IV

Cell	E (mV) $= A + BT$ (K)		Precision (mV)	T range (K)
	A	B		
I	260.26	0.1394	±4.0	880–1045
II	−9.99	0.3847	±4.0	740–800
III	288.24	0.4975	±2.0	700–800
IV	−202.4	0.2487	±4.0	850–940

3. Results and discussion

An endothermic peak recorded on a Seiko 320 model thermoanalyzer is shown in Fig. 1. Though it may appear as a second order transition, the base line tended to return to the initial level beyond 1100 K indicative of the probable sluggishness in the first order transition. The transition temperature was found to be 1060 K. The reversibility of this transition was ascertained by the occurrence of an exotherm in the cooling cycle at 1048 K. The reversibility was also checked by a second heating and cooling cycle (not shown here), but the peaks were found to be attenuated in size. It should be mentioned that these results were used only to confirm the transition temperature observed during the first heating. The transition temperature was thus found to be (1055 ± 5) K.

The emf data obtained on cells I–IV are depicted in Fig. 2. These data were subjected to least-squares regression analysis so as to yield a linear equation of the form

$$E_k \text{ (mV)} = A + BT \text{ (K)}. \tag{5}$$

The coefficients of the regression expressions for the k cells (k = I–IV) are summarized in Table 1. Each of the above four galvanic cells are reversible with respect to Na^+ by virtue of the choice of Na-β″-alumina electrolyte. The soda potential of the Na_2ZrO_3/ZrO_2 mixture in conjunction with $O_2(p_{O_2} = 1.013$ bar) sets up a sodium potential in the test electrodes of cells I and III which are higher than those established by the coexisting phase mixture in the respective reference electrodes. Therefore, these cells (including II and IV) should function as sodium concentration cells with transport with the transference number of Na^+ in Na-β″-alumina taken as unity. It could be seen from Eqs. (1)–(3) that the standard Gibbs energy change $\Delta_r G^0$ for cell III could be derived as the algebraic sum of the corresponding $\Delta_r G^0$ for cells I and II. In other words, if the cells I and II were connected in series, the resultant emf (which would be the algebraic sum of those of the emfs of cells I and II) should be equal to the directly measured values of emf of cell III at temperatures interpolated within the range of measurements.

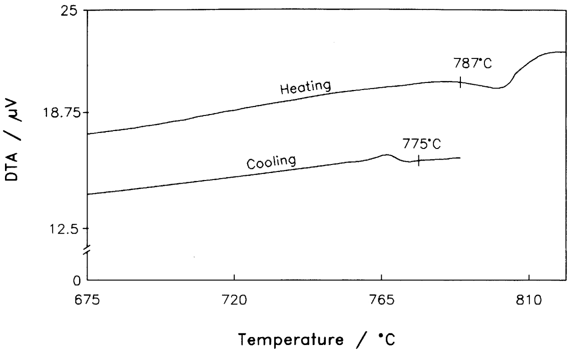

Fig. 1. DTA trace of Na_2ZrO_3 for one cycle of heating and cooling.

At this juncture, it is necessary to point out that the limits of precision (1σ, σ being standard deviation) in the regression equations for the emf results presented in Fig. 2 were adequately expanded to take care of the rather larger uncertainties in the sodium potential values for the ASBA reference electrode. As mentioned in Section 2, only the uncertainty in the emf values arising apart from other factors out of the 10% nominal variation in the mole ratio of Na_2ZrO_3 to ZrO_2 alone were taken care of; no effort to measure the scatter corresponding to a similar variation in the mole ratio of

Table 2
Internal consistency check between galvanic cells I–III (condition $E_{I} + E_{II} = E_{III}$ is fulfilled)

Cell	E (mV)		T range (K)
	800 K	900 K	
I	371.8	385.7	880–1045
II	297.9	336.3	740–800
III	686.2	735.9	700–800
$E_{I} + E_{II}$	669.7	722.0	740–1045

α-alumina to sodium-β-alumina ($NaAl_{11}O_{17}$) was attempted. Thus, the scatter in the emf expressions were of the order of <1 mV. An additional 3 mV in the precisions for cells I and II was estimated from the earlier work on the system α-Al_2O_3/$NaAl_{11}O_{17}$ [9,10]. Further, the validity of the assumption that Na-β″-alumina is a pure Na^+ conductor with negligible electronic conduction was often debated in the literature [11–13]. Therefore, polarization errors arising out of the not too insignificant electronic conduction would warrant a widening of the error band. The last mentioned factor is specifically applicable to CO_2 sensors and hence, a larger scatter (than what could be inferred from Fig. 2) was associated with E_{IV} in Table 1. The sources of error including the ones pointed in the preceding paragraph had made an internal consistency check among the results from cells I–III rather inevitable. At two interpolated temperatures of 800 and 900 K, the algebraic sum of the interpolated values of emf of cells I and II is compared with those of emf interpolated from direct experimental least-squares expression for cell III and are presented in Table 2. The agreement between say 670 mV obtained as sum of 372 and 298 mV for cells I and II at 800 K is in fair agreement with 686 mV derived from the direct least-square equation for cell III from Table 1 (shown in the last row of Table 2). This difference, which is the maximum in the temperature range of the present measurements, is within the sum of 1σ for cells I–III.

For deriving $\Delta_f G^0$ of Na_2ZrO_3 from the least-squares data listed in Table 1 in conjunction with the virtual cell reactions represented by Eqs. (1)–(4), the relevant Gibbs energy data reliably reported in the literature on ZrO_2, Al_2O_3, Na_2CO_3 and CO_2 were taken from Ref. [14]. The $\Delta_f G^0$ data for Na_2MoO_4 and $Na_2Mo_2O_7$ were taken from Ref. [6]. These calculations had led to the derivation of the linear least-squares expressions for $\Delta_f G^0$ (Na_2ZrO_3, s) whose coefficients are listed in Table 3. The least-squares expressions corresponding to No. 1 and 2 of Table 3 agree reasonably well with each other and also with that represented by No. 3 if one compares the values of $\Delta_f G^o$ derived at 900 K as shown in the last column of Table 3. However, the values of the individual slopes and intercepts of No. 1 and 2 differ considerably from those for No. 3. In view of the additional uncertainties associated with the electronic conduction in Na-β″-alumina especially in the context of CO_2 sensing, the least-squares expression for $\Delta_f G^0$ (Na_2ZrO_3, s) derived from the emf results of cell IV were used only to assess the consistency and not for deriving an expression for $\Delta_f G^0$. However, to give equal weight to all emf values from both cells I and III, the $\Delta_f G^0$ (Na_2ZrO_3, s) for each temperature of emf measurements of cells I and III was derived from the corresponding $\Delta_r G^0$ and the Gibbs energy data for each phase in the reference electrode as per virtual cell reactions (1) and (3). Thus, a new least-squares expression based on seven average emf values on cell I and eight from cell III was derived and is given by

$$\Delta_f G^0\ (Na_2ZrO_3, s) \pm 8\ \text{kJ/mol} = -1699.4 + 0.3652T\ (\text{K}) \tag{6}$$

valid over the range 700–1045 K. It should be pointed out that the standard deviation in the Gibbs energy data was adequately expanded to accommodate the uncertainties in the standard Gibbs energies for the solid phases employed in the reference/test electrodes in cells I–III. A maximum temperature of 1045 K for the emf measurements was recorded for cell I. In fact, it was observed that the emf values drifted rapidly beyond 1045 K indicative of a change in slope corresponding to a possible phase transition in Na_2ZrO_3. Due to a larger scatter, these points are omitted in Fig. 2. Taking this observation in conjunction with that on the DTA trace of the zirconate phase in Fig. 1, it is inferred that the onset of the phase transition might be taking place at 1045 K in fair agreement with 1055 K observed by employing the dynamic DTA technique. The increased drift and scatter beyond the possible onset temperature of 1045 K for the transition in Na_2ZrO_3 could not be

Table 3
Comparison of Gibbs energy data $\Delta_f G^0$ (Na_2ZrO_3, kJ/mol) obtained from the present measurements

No.	$\Delta_f G^0\ (Na_2ZrO_3, s)/\text{kJ/mol} = A + BT$ (K)		T range (K)	$\Delta_f G^0$ (900 K)/kJ/mol	Reference electrode used
	A	B			
1	−1713.9	0.3800	880–1045	−1371.9	α-Al_2O_3 + $NaAl_{11}O_{17}$
2	−1706.5	0.3749	700–800	−1369.1	$Na_2Mo_2O_4$ + $Na_2Mo_2O_7$
3	−1774.5	0.4548	850–940	−1365.2	Na_2CO_3, CO_2, O_2

corroborated by cell III whose upper temperature of measurement was only 800 K which limit was set by rather high volatility of MoO_3. For an evaluation of the consistency of the Gibbs energy results presented here, the values of -1407.2 and -1370.7 kJ/mol obtained for $\Delta_f G^0$ (Na_2ZrO_3, s) interpolated at 800 and 900 K are compared with -1424.3 and -1391.9 by Beyer et al., -1397.5 and -1362.6 by Iyer et al., respectively. The present results are thus found to be intermediate between the two pairs of literature data and therefore, the $\Delta_f G^0$ expression given by Eq. (6) could be taken as a better representation of the hitherto reported data on Na_2ZrO_3.

4. Conclusion

The present investigation on the high temperature stability of Na_2ZrO_3 over the range 700–1045 K is considered as more reliable owing to the use of three different reference electrodes for fixing the sodium potentials, which facilitated internal consistency checks. The data were also found to be consistent with those reported in the literature. Though no numerical expression for the standard Gibbs energy change for the phase transition in Na_2ZrO_3 taking place at or above 1045 K could be directly measured by emf, the scatter in data on cell I beyond this temperature corroborated by a sluggish endotherm in DTA at (1055 ± 5) K confirms the occurrence of a first order phase change between 1045 and 1055 K. Hence, it is suggested that while high temperature XRD taken at close intervals between 1000 and 1100 K would pinpoint the transition temperature, drop calorimetry will help to give quantitative enthalpy data.

Acknowledgements

The authors are deeply indebted to Dr V.S. Raghunathan, Associate Director, Materials Characterization Group, IGCAR, Kalpakkam and Dr Baldev Raj, Director, MCRG, IGCAR, Kalpakkam for their keen interest and constant encouragement throughout the course of investigation. The authors are also grateful to Dr R. Pankajavalli for recording the DTA pattern of the sample.

References

[1] H. Kleykamp, J. Nucl. Mater. 131 (1985) 221.
[2] R.P. Beyer, K.O. Bennington, R.R. Brown, J. Chem. Thermodyn. 17 (1985) 11.
[3] J. Maier, U. Warhus, J. Chem. Thermodyn. 18 (1986) 309.
[4] V.S. Iyer, V. Venugopal, S. Mohapatra, Z. Singh, K.N. Roy, R. Prasad, D.D. Sood, J. Chem. Thermodyn. 20 (1988) 781.
[5] R. Kohli, Thermochim. Acta 65 (1983) 285.
[6] T. Mathews, D. Krishnamurthy, T. Gnanasekaran, J. Nucl. Mater. 247 (1997) 280.
[7] R. Subasri, O.M. Sreedharan, Mater. Lett. 30 (1997) 289.
[8] O.M. Sreedharan, M.S. Chandrasekharaiah, M.D. Karkhanavala, High Temp. Sci. 9 (1977) 109.
[9] R. Subasri, O.M. Sreedharan, Solid State Ionics 93 (1997) 341.
[10] K.T. Jacob, K. Swaminathan, O.M. Sreedharan, Electrochim. Acta 36 (1991) 791.
[11] H. Näfe, S. Gollhofer, F. Aldinger, Proc. MRS 548 (1999) 521.
[12] H. Näfe, Solid State Ionics 115 (1998) 205.
[13] H. Näfe, J. Electrochem. Soc. 143 (1996) 943.
[14] O. Knacke, O. Kubaschewski, K. Hesselmann (Eds.), Thermochemical Properties of Inorganic Substances, Springer, Berlin, 1991.